Hopf Bifurcation in Acoustically Excited Faraday Ripples on a Bubble Wall

Alexey O. Maksimov[a], Koen Winkels[b†], Peter R. Birkin[c] and Timothy G. Leighton[d]

[a]*V.I. Il'ichev's Pacific Oceanological Institute, FEBRAS, Vladivostok 690041, Russia*
[b]*Faculty of Science and Technology University of Twente 7500 AE Enschede, The Netherlands*
[c]*School of Chemistry and* [d]*Institute of Sound and Vibration Research, University of Southampton, Highfield, Southampton SO17 1BJ, UK*

Abstract. Observations of surface waves on the wall of a bubble which is subjected to an acoustical field demonstrate differences in the transient processes, as well as a marked variation in steady state amplitudes, that depend on the insonification conditions. To clarify these observations, the stability analysis of the system has been carried out and the presence of the Hopf bifurcation was established. The appearance of the limiting circle corresponds to the presence of periodic variations in the amplitudes of interacting breathing (volume) and distortion (surface) modes. Comparison between observation and modeling indicate qualitative similarities, for example in that the oscillations will be seen for sufficiently high pressure amplitudes and will be absent at the bottom of the threshold curve for the excitation of the ripples.

Keywords: Bubble, Faraday ripples, Hopf bifurcation

PACS: 43.25.Yw, 47.20.Ky, 47.55.dd

INTRODUCTION

The nonlinear response of a gas bubble to a low frequency ω acoustic wave results in parametrically-generated shape oscillations above a well defined threshold. This effect (the generation of surface waves under the acceleration in the plane normal to a liquid\gas interface) was first characterized 177 years ago by Faraday [1]. More recently, Ramble *et al.* [2] have discovered that there exists a significant difference in the transient times taken to establish steady-state subharmonic and fundamental combination frequency signals (the so-called 'ring-up' times) which reflect the times taken to establish surface wave activity. The theory for the transient processes near the threshold has been derived in reference [3]. In this domain, one of the eigenvalues of the linear stability problem is small (it equals zero at the threshold). The growth of instability is very slow here, causing the transient processes to be of very long duration. Subsequent studies of this effect by an acoustoelectrochemical technique (see review [4]) indicated discrepancies between experimental observation and the theory, thus motivating the photographic current study to obtain a better insight into the phenomenon.

† The contribution made by Mr Winkels was undertaken whilst he worked as an intern at ISVR, University of Southampton.

CP1022, *Nonlinear Acoustics—Fundamentals and Applications (ISNA 18), 18th International Symposium*
edited by B. O. Enflo, C. M. Hedberg, and L. Kari

INVESTIGATION OF THE RISE-TIME OF FARADAY RIPPLES

Surface waves on a bubbles were photographed at framing rates of 12000 frames per second, using a Photron APX-RS camera (the shutter time and the maximum resolution for this recording speed were 1/12000 s and 512×384 pixels respectively). A calibrated hydrophone (Brüel& Kjær type 8103), with a measuring frequency range from 0.1 Hz to 180 kHz and a receiving sensitivity of 1 V/μPa, provided measurements of the sound field.

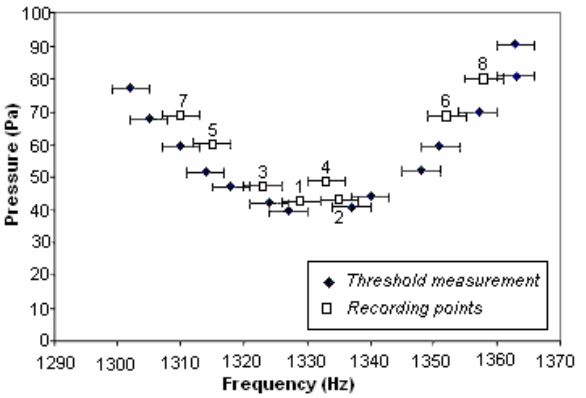

FIGURE 1. For of an air bubble of equilibrium radius $R_0 = 2.224 \pm 0.118$ mm, the figure shows the points at which the high speed recordings were taken (□). Also the driving pressure threshold points (♦) are shown for the onset of surface waves on a bubble wall for a given driving frequency $\omega/2\pi$.

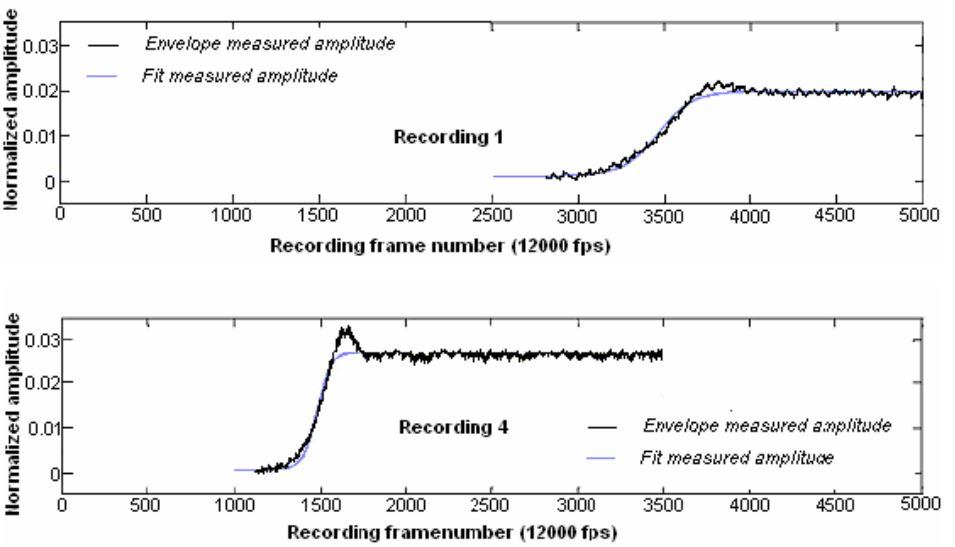

FIGURE 2 Showing the measured evolution of surface wave amplitudes on the bubble with $R_0 = 2.224 \pm 0.118$ mm (in black) and the fit of measured amplitude (in light). The driving pressure and frequency were: recording 1 – 42.6 Pa and 1329 Hz; recording 4 – 48.8.9 Pa and 1333 Hz.

Recordings of the growth of surface waves were taken for the insonification conditions labeled in Figure 1, and by subtracting the wall positions in the images, the normalized surface wave amplitude was generated (Figure 2). For tracking the bubble wall movement, the program follows a certain intensity level at particular points at the bubble interface and records its position in time (frame numbers). In some graphs there appears a clear 'overshoot' of the surface wave amplitude before reaching the steady state and subsequent variations in the steady state amplitude. The evolution of the distortion mode largely depends on the conditions relative to the threshold, affecting the characteristics as ring-up time and the steady-state amplitude.

HOPF BIFURCATION

To propose an explanation for the observed evolution of the distortion modes shown in the Figures 1 and 2, the approach derived in [3] has been used. If (ω_0, γ_0) and (ω_l, γ_l) are the natural circular frequencies and damping of the breathing mode and the distortion mode of order l respectively, then the experimental conditions examine the following two near-resonant interactions: $\omega \approx \omega_0$ and $\omega_0 \approx 2\omega_l$. In such circumstances, the slowly varying complex amplitudes of the breathing a_{00} and distortion modes a_{lm} (having the normalization of square root of action) satisfy the equations [3], which at the time scale $t\gamma_l >> 1$ have the form:

$$\dot{S} = 2\left[\mathrm{i}\left(\omega_l - \omega/2\right) - \gamma_l\right]S + 4\mathrm{i}Q_l a_{00} \mid S \mid, \quad S = \sum_{m=-l}^{l} (-1)^m a_{lm} a_{l-m} \tag{1}$$

$$\dot{a}_{00} = \left[\mathrm{i}\left(\omega_0 - \omega\right) - \gamma_0\right]a_{00} + \mathrm{i}Q_l S + \sqrt{\pi} R_0^2 P_m \left(2\rho_0 R_0^3 \omega_0\right)^{-1/2}.$$

Here the indexes correspond to the expansion of the bubble wall displacement in spherical harmonics Y_{lm}; $Q_l = (2^5\pi)^{-1/2}(4l-1)\omega_0\left(\rho_0 R_0^3 \omega_0\right)^{-1/2} R_0^{-1}$ is the coupling coefficient, S is the collective variable, P_m is the amplitude of the sound field and ρ_0 is the equilibrium density of the liquid. The stationary states are realized when the right hand sides of equations (1) become zero. Stability analysis leads to the following equation for eigenvalues

$$\lambda^4 + a_1\lambda^3 + a_2\lambda^2 + a_3\lambda + a_4 = 0, \tag{2}$$

where $a_1 = 2(\gamma_0 + \gamma_l)$, $a_2 = [(\omega_0 - \omega)^2 + \gamma_0^2] + 4 \mid S \mid_* + 4\gamma_0\gamma_l$, $a_3 = 2\gamma_l[(\omega_0 - \omega)^2 + \gamma_0^2]$ $+4 \mid S \mid_* (\gamma_0 + \gamma_l)$, $a_4 = 4 \mid S \mid_* \{[\gamma_0\gamma_l - (\omega_0 - \omega)(\omega_l - \omega/2) + \gamma_0^2] + \mid S \mid_*\}$, $\mid S \mid_* = \left(2Q_l^2\right)^{-1}$ $\times\left\{\left[\left(\omega_l - \omega/2\right)\left(\omega_0 - \omega\right) - \gamma_l\gamma_0\right] \pm \sqrt{\left(P_m Q_l^0 / 2\rho_0\omega_0 R_0\right)^2 - \left[(\omega_0 - \omega)\gamma_l + (\omega_l - \omega/2)\gamma_0\right]^2}\right\}$.

The Routh–Hurwitz stability criterion:

$$a_4 > 0,\ a_3 > 0,\ a_2 > 0,\ a_3\left(a_2 a_1 - a_3\right) - a_4 a_1^2 > 0 \tag{3}$$

is always satisfied for the second and third conditions. The vanishing of the first condition $a_4 = 0$ $(\lambda = 0)$ determines the transcritical bifurcation and has been analyzed in [3]. The vanishing of the last condition $a_3\left(a_2 a_1 - a_3\right) - a_4 a_1^2 = 0$ leads to

the Hopf bifurcation in which a fixed point of a dynamical system loses stability as a pair of complex conjugate eigenvalues of the linearization around the fixed point cross the imaginary axis of the complex plane. The Hopf bifurcation can occur if a slight phase mismatch is allowed, i.e. $(2\omega_l - \omega_0)^2/16 > \gamma_0(\gamma_l + \gamma_0/2)$. This type of bifurcation was detected in numerical calculations of Mei and Zhou [5] for a simplified axi-symmetric model. Calculated with standard parameter values, the thresholds for transcritical (corresponding to the excitation of the distortion modes) and Hopf bifurcations are shown in Figure 3.

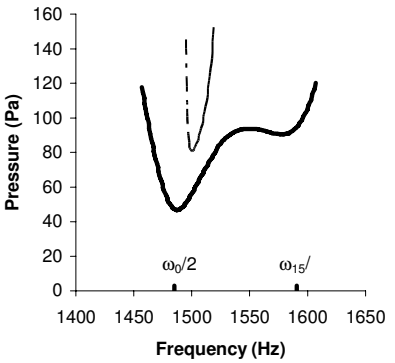

FIGURE 3. The thresholds for transcritical (solid line) and Hopf (dashed line) bifurcations calculated with standard parameter values: $\gamma = 1.402$ – polytropic exponent; $\sigma = 7.2 \cdot 10^{-2}$ Nm – surface tension (water/air 20°C), $P_0 = 1.02 \cdot 10^5$ Pa – ambient pressure; $\rho_0 = 998$ kg/m^3 – equilibrium water density; $R_0 = 2.224 \cdot 10^{-3}$ m – equilibrium bubble radius: $c = 1484$ m/s – sound speed in water, $\nu = 1.004 \cdot 10^{-6}$ m^2/s – kinematic viscosity; $D = 2 \cdot 10^5$ m^2/s – diffusion coefficient; $l = 15$ – mode number.

The normal form for the transcritical and Hopf bifurcations, which govern the evolution of 'the parameter of order', are derived by central manifold reduction and subsequent nonlinear transformation of the initial system (1). Specifically, the solution for the transcritical bifurcation has two plateaus (at $t \to 0$ and at $t \to \infty$) separated by an S-curve, and thus qualitatively reproduces the main features seen in the evolution of the distortion mode amplitude shown in Figure 2. The appearance of the limit circle means periodic variation in the amplitudes of the parametrically interacting breathing (volume) and distortion (surface) modes. Comparison between observation and modeling indicates this qualitative similarity, for example in that the oscillations will be seen for sufficiently high pressure amplitudes and will be absent at the bottom of the threshold curve for the excitation of the distortion modes.

REFERENCES

1. M. Faraday, *Philos. Trans. R. Soc. London* **121,** 319-340 (1831).
2 D. Ramble, A. Phelps, and T.G. Leighton, *ACUSTICA acta acustica* **84**, 986-988 (1998).
3. A.O. Maksimov, T.G. Leighton, *ACUSTICA-acta acustica* **87**, 322-332 (2001).
4 T. G. Leighton, *Int. J. Mod. Phys. B* **18,** 3267-3314 (2004).
5 C. C. Mei and X. Zhou, *J. Fluid Mech.* **229**, 29-50 (1991).